

Computational Investigation on Structural and Physical Properties of AIN Nanosheets and Nanoribbons

Yafei Li, Zhenyu Yang, Zheng Chen, and Zhen Zhou*

Institute of New Energy Material Chemistry, College of Chemistry, Institute of Scientific Computing, Nankai University, Tianjin-300071, P. R. China

Through first-principles computations, we investigated the structural, electronic and magnetic properties of two-dimensional AIN single layer and one-dimensional AIN nanoribbons. AIN single layer and nanoribbons quit the Wurtzite configuration and adopt a graphitic-like structure after geometry optimization. Both hydrogen-terminated zigzag and armchair AIN nanoribbons have a direct band gap, which increases monotonically with increasing ribbon width. Bare zigzag AIN nanoribbons have a spin-polarized ground state and are magnetic semiconductors. The results may promote the experimental preparation of AIN nanosheets and nanoribbons and their applications to nanotechnology.

Keywords: AIN, Nanosheet, Nanoribbon, First Principles, Band Structure.

1. INTRODUCTION

In recent years, the successful experimental realization of graphene (actually a single layer of graphite)¹ and its excellent properties have attracted great research interest in two-dimensional (2-D) layer materials. When graphene is further reduced into one-dimensional (1-D) graphene nanoribbons (GNRs), some more intriguing properties emerge. Through first-principles computations, Son et al.² demonstrated that GNRs with zigzag or armchair edges both have a nonzero energy gap, which was confirmed experimentally later.3 Fujita et al.4 demonstrated previously that zigzag GNRs have special localized edge states, which are ferromagnetically ordered but have opposite spin directions between two edges. Recent studies have disclosed that external transverse electronic field⁵ or proper edge modifications, 6,7 can result in half-metallicity in zigzag graphene nanoribbons, which would find potential applications in spintronic devices.

Following the intensive studies on GNRs, recently, the sheet and ribbon structures of inorganic materials, such as BN,⁸⁻¹⁰ SiC,¹¹ ZnO,¹² and MoS₂,¹³ have also been explored theoretically, and many interesting properties are found in these systems. Closely related to BN and ZnO, AlN also attracts our interest. AlN is an important III–V wide-band-gap (~6.2 eV) semiconductor with potential use in electronic and light emitting devices. Unlike BN, whose stable phase is layered hexagonal

structure, AlN usually crystallizes in Wurtzite phase as ZnO, where Al and N atom all adopt sp^3 -hybridization. The experimentally realized AlN nanotubes¹⁴ have the faceted geometry with hexagonal cross sections. The following first-principles computations¹⁵⁻¹⁹ confirmed that the sp³-hybridized faceted model of AlN nanotubes is energetically more favorable than the sp²-hybridized cylindrical one. However, the sp^2 -hybridized AlN structures are not hence excluded in nanoscale. Freeman et al.20 have demonstrated that thinner Wurtzite AIN films could remove the dipole and adopt a graphitic-like structure. The recent experimental observation of depolarized ZnO (0001) monolayer²¹ makes us confident in obtaining planar structures of AlN. Very recently, Du et al. 22 have reported the geometric and electronic structures of AlN nanoribbons based on density functional theory (DFT) computations; in their work, only a zigzag AlN nanoribbon with width parameter $N_z = 10$ was studied, and some important issues are still pending. What about the geometric and electronic properties of 2-D AlN single layer? What are the electronic properties of armchair AlN nanoribbons? How do the electronic properties of AlN nanoribbons vary as a function of ribbon width? In this work, detailed DFT computations were carried out to address the above questions.

2. COMPUTATIONAL DETAILS

Spin-polarized first-principles computations were performed with the plane-wave pseudopotential technique

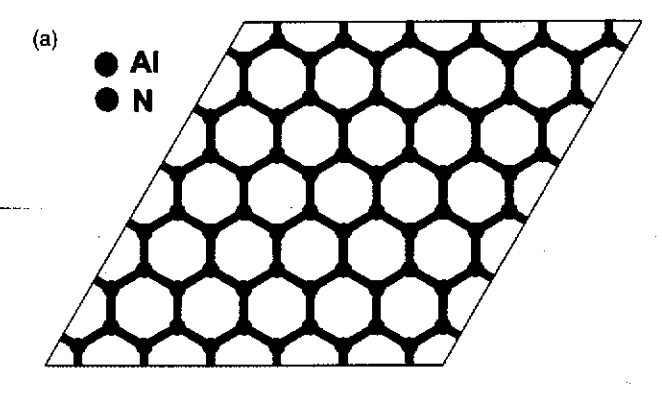
^{*}Author to whom correspondence should be addressed.

implemented in the Vienna ab initio simulation package (VASP).23.24 The generalized gradient approximation (GGA) with the PW91 functional.²⁵ and a 360 eV cutoff for the plane-wave basis set were adopted in all the computations. The electron-ion interactions were modeled using the projector augmented wave (PAW) approach, ^{26,27} and the following electronic states were treated as valence: Al $3s^23p^1$, N $2s^22p^3$, and H $1s^1$. The supercell is large enough (the vacuum space at least 12 Å) to ensure that the interaction between nanosheets/ribbons and their periodic images can be safely avoided. Five Monkhorst-Pack special k points were used for sampling the 1-D Brillouin zone, and the convergence threshold was set as 10⁻⁴ eV in energy and 10^{-3} eV/Å in force. The positions of all the atoms in the supercell were fully relaxed during the geometry optimizations. On basis of the equilibrium structures, 21 k points were then used to obtain band structures.

3. RESULTS AND DISCUSSION

3.1. AlN Single Layer

Firstly, we studied the structural and electronic properties of AlN single layer. The infinite 2-D structure cut from the polar (0001) sheet of bulk AlN is displayed in Figure 1(a). The slab includes 32 Al and 32 N atoms. After the full



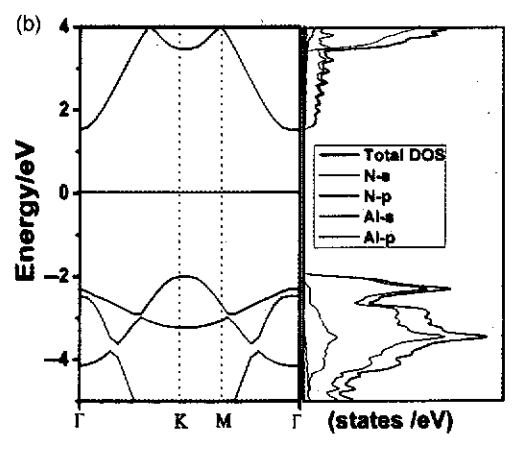


Fig. 1. Optimized structure (a) and computed band structure and density of states (b) of 2-D AlN sheet. Al and N atoms are denoted with purple and blue balls, respectively.

structural relaxation, the polar (0001) sheet changed into a smooth one, and Al and N atoms are entirely located in the same plane and adopt the sp^2 hybridization. Similar phenomena have also been found in other planar structures of Wurtzite materials. 19,28 The Al-N bond length is 1.80 Å, and Al-N-Al (N-Al-N) bond angle is 120°. The Mulliken charge population analysis shows that the amount of charge transfer from Al to N is 0.98 |e|, indicating the strong ionicity of Al-N bonds. According to our computation level, AIN single layer is semiconducting with a 3.60 eV band gap (the computed band gap for bulk AlN is 4.92 eV at the same theoretical level). Here note that DFT usually underestimates the band gap. To get more insight, we computed the total density of states (TDOS) and partial density of states (PDOS) of AlN single layer. As shown in Figure 1(b), the valence band maximum (VBM) mainly comes from the electron pairs localized at the N atoms, while the conduction band minimum (CBM) consists mainly of Al 3s orbital.

3.2. H-Terminated AlN Nanoribbons

From 2-D AlN single layer, we can obtain zigzag and armchair nanoribbons by cutting along two different directions. Similar to GNRs^{2,4-6} and other inorganic nanoribbons, 8,13 the width parameter N_z (N_a) of AlN nanoribbons is defined as the number of zigzag lines (dimmer lines) across the ribbon width. The edge twocoordinated Al and N atoms are all saturated with H atoms to hold the sp^2 -hybridization. Figure 2 shows the optimized configurations of H-terminated 8-zAINNR and 12-aAlNNR, with ribbon widths of 19.83 and 17.05 Å, respectively. For both ribbons, the average Al-N bond length is 1.80 Å, which equals to that of AlN single layer. The Al-H and N-H bond lengths are 1.58 and 1.02 Å, respectively. There is no obvious structure reconstruction at the ribbon edges. To determinate the ground state of AlN nanoribbons, we performed spin-polarized computations for both zigzag and armchair AlN nanoribbons, and found that the energies are the same as those from spinnonpolarized computations. Therefore, the ground state of H-terminated AlN nanoribbons can be regarded as spinnonplarized one.

On basis of the optimized structures, we computed the band structures for H-terminated 8-zAlNNR and 12-aAlNNR. As displayed in Figure 2, both 8-zAlNNR and 12-aAlNNR are semiconducting with a direct band gap of 3.33 and 3.71 eV, respectively. The valence and conduction band edge are both located at the Γ point. The direct band gap suggests that AlN nanoribbons could be used for optoelectronics. We computed the partial charge densities associated with the VBM and the CBM of these two nanoribbons. As shown in Figure 2(a), for 8-zAlNNR, the VBM is an edge state with wave function localized at the edge N atoms. In contrast, the CBM consists mainly

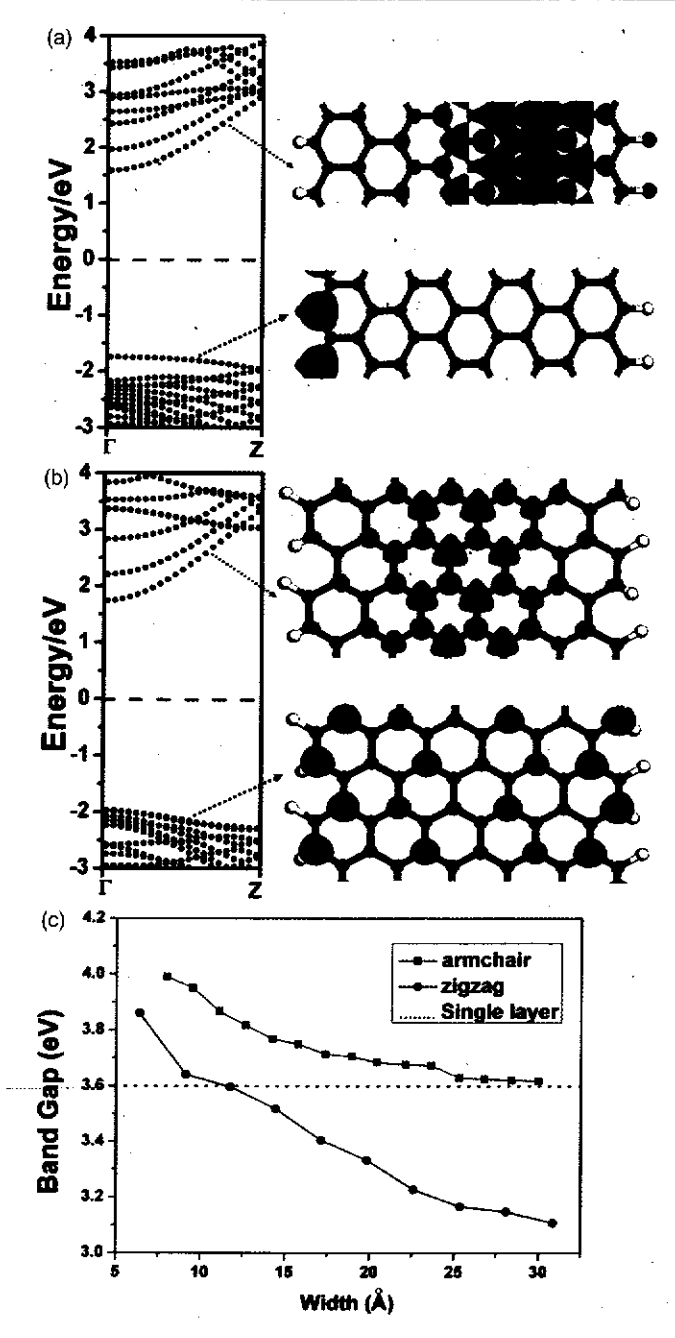


Fig. 2. Band structures (left) and charge densities of VBM (right lower) and CBM (right upper) for H-terminated 8-zigzag (a) and 12-armchair AlN nanoribbons (b). (c) Variation of the band gap of zigzag ($3 \le N_z \le 12$) and armchair ($6 \le N_z \le 20$) AlN nanoribbons as a function of ribbon width.

of the states of inner N and Al atoms. For 12-aAlNNR (Fig. 2(b)), the VBM mainly consists of the state of N atoms throughout the ribbon, while the CBM comes from the state of inner N and Al atoms. The above results imply that edge atoms should play an important role of the electronic properties of AlN nanoribbons.

Figure 2(c) presents how band gap varies as a function of ribbon width for a series of H-terminated AlN nanoribbons. The ribbons studied here all have wide band

gaps. For both zigzag and armchair nanoribbons, the band gap decreases monotonically with increasing ribbon width due to the quantum confinement effect. The band gap of aAlNNRs converges to the value of AlN single layer (3.60 eV) gradually with the increase of ribbon width. However, for zAlNNRs, when the ribbon width is greater than 9.11 Å $(N_z > 4)$, the band gap is smaller than that of AlN single layer, which should be contributed to edge state effect, as shown in Figure 2(a).

3.3. Bare Zigzag AlN Nanoribbons

Also, we investigated the electronic properties of bare zigzag AlN nanoribbons. Here three kinds of zigzag 8-zAlNNR were compared: the fully bare 8-zAlNNR, 8-zAlNNR with one bare N edge and one passivated Al edge (8-zAlNNR-AlH), and 8-zAlNNR with one bare Al edge and one passivated N edge (8-zAlNNR-NH).

Firstly, as shown in Figure 3(a) the magnetic ground state of fully bare 8-zAlNNR is antiferromagnetic at the Al edge and ferromagnetic at the N edge, which is quite similar to fully bare zigzag BN nanoribbons. 29,30 Compared with H-terminated 8-zAlNNR, fully bare 8-zAlNNR shows asymmetrical spin-up and spin-down bands (Fig. 4(a)), which means that the spin degeneracy has been broken. Each spin channel shows semiconducting characteristic; the band gaps are 1.50 and 0.26 eV for spin-up and spin-down channel, respectively. For 8-zAlNNR-AlH, the magnetic ground state is ferromagnetic at the N edge and nonmagnetic at the Al edge (Fig. 3(b)). Figure 4(b) presents the spin-resolved band structure of 8-zAlNNR-AlH, which shows a spin-splitting behavior with an indirect band gap of 2.93 and 0.61 eV for

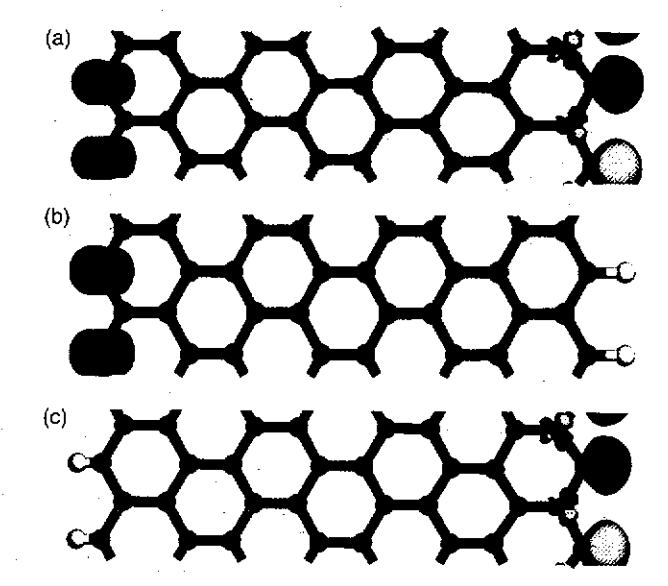


Fig. 3. Spatial spin distribution (up-down) of the fully bare 8-zAlNNR (a), 8-zAlNNR with one bare N edge and one passivated Al edge (b), and 8-zAlNNR with one bare Al edge and one passivated N edge (c). The isovalues for the green and yellow isosurfaces are 0.02 and -0.02 e/Å^3 , respectively.

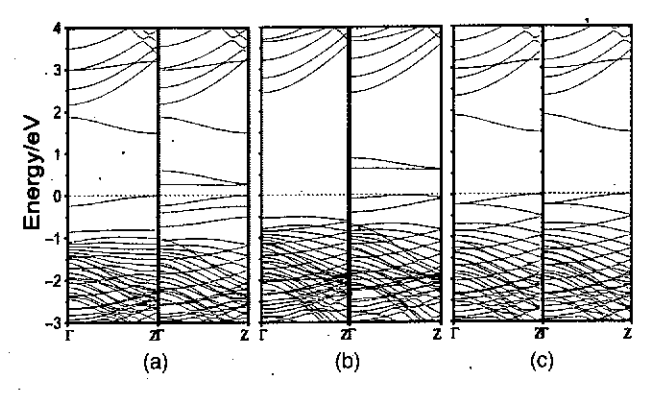


Fig. 4. Computed spin-polarized band structure for the fully bare 8-zAINNR (a), 8-zAINNR with one bare N edge and one passivated Al edge (b), and 8-zAINNR with one bare Al edge and one passivated N edge (c). (left: spin-up; right: spin-down).

spin-up and spin-down channel, respectively. The magnetic ground state for 8-zAlNNR-NH is antiferromagnetic at the Al edge and nonmagnetic at the N edge (Fig. 3(c)). As shown in Figure 4(c), the spin-up and spin down channels for 8-zAlNNR-NH are fully degenerate and both have a 1.49 eV direct band gap, which is much lower than H-terminated 8-zAlNNR (3.33 eV, Fig. 2(a)).

4. CONCLUSION

In summary, we have investigated the structural and electronic properties of two- and one-dimensional planar honeycomb AlN structures with density functional theory computations. 2-D AlN single layer adopts planar structure similar to graphene, and the strong ionicity of between Al and N results in a wide band gap. When 2-D AlN single layer is cut into 1-D AlN nanoribbons, both zigzag and armchair AlN ribbons with hydrogen-terminated edges are nonmagnetic and have a direct band gap, which decreases with the increase of ribbon width. Especially, the band gap of wider zigzag AlN nanoribbons is even narrower than that of AlN single layer, which is attributed to edge states. The bare zigzag AlN nanoribbons are spin-polarized, and the magnetic ground state and electronic properties are strongly dependent on whether Al or N edge is passivated. The feasible tuning of the electronic and magnetic properties of AlN nanosheets and nanoribbons may be useful for their application in nanotechnology.

Acknowledgment: This work was supported by the Undergraduate Research Funding of Nankai University, the NSFC (20873067) and NCET (08-0293) in China.

References and Notes

- K. S. Novoselov, A. K. Geim, S. V. Morozov, D. Jiang, Y. Zhang, S. V. Dubonos, I. V. Grigorieva, and A. A. Filrsov, *Science* 306, 666 (2004).
- Y. W. Son, M. L. Cohen, and S. G. Louie, *Phys. Rev. Lett.* 97, 216803 (2006).
- 3. X. L. Li, X. R. Wang, L. Zhang, S. W. Lee, and H. J. Dai, *Science* 319, 1229 (2008).
- M. Fujita, K. Wakabayashi, K. Nakada, and K. Kusakabe, J. Phys. Soc. Jpn. 65, 1920 (1996).
- Y. W. Son, M. L. Cohen, and S. G. Louie, *Nature (London)* 444, 347 (2006).
- E. J. Kan, Z. Li, J. Yang, and J. G. Hou, J. Am. Chem. Soc. 130, 4224 (2008).
- Y. F. Li, Z. Zhou, P. W. Shen, and Z. F. Chen, ACS Nano 3, 1952 (2009).
- 8. C.-H. Park and S. G. Louie, Nano Lett. 8, 2200 (2008).
- X. F. Gao, Z. Zhou, Y. L. Zhao, S. Nagase, S. B. Zhang, and Z. F. Chen, J. Phys. Chem. C 112, 12677 (2008).
- Y. Ding, Y. L. Wang, and J. Ni, Appl. Phys. Lett. 94, 233107 (2009).
- L. Sun, Y. F. Li, Z. Y. Li, Q. X. Li, Z. Zhou, Z. F. Chen, J. L. Yang, and J. G. Hou, J. Chem. Phys. 129, 174114 (2008).
- A. R. Botello-Méndez, F. López-Urías, M. Terrones, and H. Terrones. Nano Lett. 8, 1562 (2008).
- Y. F. Li, Z. Zhou, S. B. Zhang, and Z. F. Chen, J. Am. Chem. Soc. 130, 16739 (2008).
- Q. Wu, Z. Hu, X. Z. Wang, Y. N. Lu, X. Chen, H. Xu, and Y. Chen. J. Am. Chem. Soc. 125, 10176 (2003).
- X. Chen, J. Ma, Z. Hu, Q. Wu, and Y. Chen, J. Am. Chem. Soc. 127, 7982 (2005).
- Z. Zhou, J. J. Zhao, Y. S. Chen, P. V. R. Schleyer, and Z. F. Chen. Nanotechnology 18, 424023 (2007).
- M. W. Zhao, Y. Y. Xia, X. D. Liu, Z. Y. Tan, B. D. Huang, C. Song, and L. M. Mei, J. Phys. Chem. B 110, 8764 (2006).
- Y. F. Li, Z. Zhou, P. W. Shen, S. B. Zhang, and Z. F. Chen, *Nanotechnology* 20, 215701 (2009).
- 19. Y. F. Li, Z, Zhou, Y. S. Chen, and Z. F. Chen, *J. Chem. Phys.* 130, 204706 (2009).
- C. L. Freeman, F. Claeyssens, N. L. Allen, and J. H. Harding, *Phys. Rev. Lett.* 96, 066102 (2006).
- C. Tusche, H. L. Meyerheim, and J. Kirschner, *Phys. Rev. Lett.* 99, 026102 (2007).
- A. J. Du, Z. H. Zhu, Y. Chen, G. Q. Lu, and S. C. Smith, *Chem. Phys. Lett.* 469, 183 (2009).
- G. Kresse and J. Hafner, J. Phys.: Condens. Matter. 6, 8245 (1994).
- 24. G. Kresse and J. Hafner, Phys. Rev. B 49, 14251 (1994).
- 25. J. P. Perdew and Y. Wang, Phys. Rev. B 45, 13244 (1992).
- 26. P. E. Blöchl, Phys. Rev. B 50, 17953 (1994).
- 27. G. Kresse and D. Joubert, Phys. Rev. B 59, 1758 (1999).
- Z. Zhou, Y. F. Li, L. Liu, Y. S. Chen, S. B. Zhang, and Z. F. Chen, J. Phys. Chem. C 112, 13926 (2008).
- 29. V. Barone and J. E. Peralta, Nano Lett. 8, 2210 (2008).
- F. W. Zheng, G. Zhou, Z. R. Liu, J. Wu, W. H. Duan, B.-L. Gu, and S. B. Zhang, *Phys. Rev. B* 78, 205415 (2008).

Received: 4 September 2009. Accepted: 30 October 2009.